A Fast Method to Measure Trabecular Bone Thickness Anisotropy

B. Vasilic[1], F. W. Wehrli[1]

[1]Laboratory for Structural NMR Imaging, Department of Radiology, University of Pennsylvania Medical Center, Philadelphia, PA, United States

INTRODUCTION

The direction and intensity of loads experienced by the skeleton results in anisotropic micro-structure of trabecular bone (TB) (Wolff's law [1]). Both, disease and aging significantly influence the degree of anisotropy. A fast and accurate means to measure the anisotropy of the TB micro-structure would provide a quantitative way to follow changes during disease progression or therapeutic intervention. Measuring TB anisotropy using in-vivo micro-MRI is a challenging goal not yet achieved with accuracy sufficient to detect changes in individual subjects. The autocorrelation function (ACF) of the MR signal, through its full width at half maximum (FWHM), can be used to estimate the mean TB thickness [2] along different directions. The ACF can be robustly determined in MR experiments since its Fourier transform is the power spectrum of the *k*-space data, i.e. the square of its absolute value. Therefore, translational motion of the subject during acquisition, producing only changes in the phase of the signal, has no effect on the ACF. Of particular interest to us are the principal values of the thickness anisotropy tensor. The principal values can be determined as the extrema of the thickness as a function of the direction along which it is measured. The directions for which the thickness reaches such extrema are called principal directions. Because the principal directions are extremal the mean thickness varies slowly around them. Thus, the anisotropy tensor, as determined from the ACF, is also robust to rotations that only weakly influence the measured values of the thickness along the principal directions. Robustness to noise is another advantage of the ACF. The main effect of noise in the signal on the ACF is a delta function the center of image space because the autocorrelation of white noise is a delta function. This artifact can be removed in post-processing allowing for automatic determination of the FWHM from very noisy data.

It can be shown that the FWHM principal values, because of the special properties of the principal directions, can be measured with high accuracy from scans that have a very low resolution in the direction perpendicular to the principal direction. Here we demonstrate a fast anisotropic autocorrelation readout technique (FAAR) in which the principal values of the ACF FWHM are measured quickly and accurately by three anisotropic 3D rectilinear scans. Each scan has a high resolution readout acquired parallel to a previously determined principal direction with low resolution phase encodings in the remaining two perpendicular directions. We show that the principal values determined in this way are robustly accurate to a reduction of the resolution in the directions perpendicular to the principal direction.

METHODS

An inner volume imaging method was implemented on a 1.5T Siemens Sonata scanner based on volume selection followed by a 3D gradient-echo sequence (Fig. 1). A hard 90º excitation was followed by 3 pairs of adiabatic *sech* pulses each of which dephased the magnetization outside of a slice determined by its slice selection gradient. The result is a cubic subvolume of excited magnetization that was then imaged using a standard rectilinear gradient-echo acquisition. The effectiveness of adiabatic volume selection depends critically on the moments of crusher gradients applied along with each adiabatic pulse. We applied crushers with a moment of 60 mT/m · ms. The time from the initial excitation to the center of the acquisition window was 58ms. The acquisition dwell time was 0.4ms. Each adiabatic pulse lasted 2.8ms and the repetition time was 100ms.

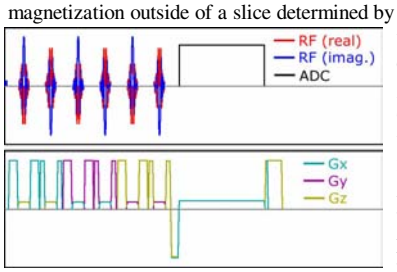

Fig 1. FAAR pulse sequence consisting of adiabatic volume selection followed by anisotropic rectilinear gradient echo acquisition.

A phantom with periodic signal-producing inclusions consisting of 9 acrylic plates, held together by a vice-like mechanism, was constructed. Four of the plates had periodically placed holes of a rounded square shape, Fig. 2a), filled with soybean oil. The nominal thickness of these plates was 8mm and the nominal dimensions of the holes was 3mm x 6mm. The plates containing the oil inclusions were spaced by 3 solid plates of 10mm nominal thickness. This set of 7 plates was compressed on each side by a solid acrylic plate. The above phantom was imaged using the previously described sequence. A cube with 4cm sides was excited and imaged, Fig. 2b, with a $(4\text{cm})^3$ field of view and acquisition matrix of 64^3 points (voxel size of $(625\mu\text{m})^3$). The scan lasted 6 min 50 s. The principal axes of the phantom were aligned with the *x*, *y* and *z* gradient axes.

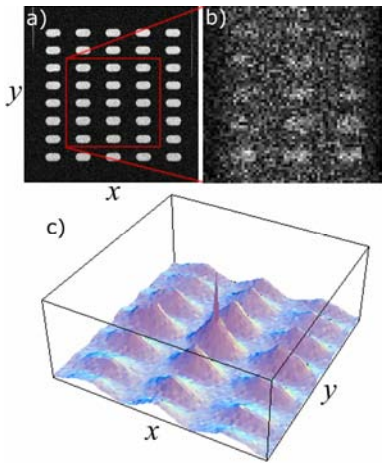

Figure 2. a) A cross-section through one of the phantom plates showing the oil inclusions acquired using a product 2D spin-echo sequence.
b) One slice reconstructed from the high resolution FAAR acquisition. The voxel size was $(625\mu\text{m})^3$.
c) The ACF at z=0 corresponding to the acquisition shown in b).

RESULTS

Even though the reconstructed images have a signal to noise ratio (SNR) of order 1, Fig. 2b), the ACF clearly shows the periodicity and anisotropy of the oil inclusions, Fig. 2c). The noise "spike" at the center of the ACF can also clearly be seen. To simulate lower resolution scans the high resolution *k*-space data was filled with zeros for $|k_i|>k_{max}$,where k_i corresponds to the two lower resolution directions and k_{max} corresponds to the low-resolution linear voxel dimension. Fig. 3a) shows the dependence of the ACF FWHM as measured from data in which the high resolution direction was parallel to one of the principal directions as the voxel size in the perpendicular plane was increased. The current version of our analysis software, written in Mathematica, does not remove the central noise peak in *sinc* interpolated images, as the lower resolution ones used here. This produces the curvature at smaller voxel sizes in Fig. 3a) since those voxels sizes correspond to lower SNRs and a more pronounced noise peak in the ACF that leads to an underestimate of the FWHM relative values corresponding to high SNR (large voxel size). This is a technical problem that can be solved by more sophisticated processing. The important conclusion is that the principal values do not change significantly even if the voxel size in the low resolution plane is reduced by 16x16=256 times. The standard deviation relative to the mean of the FWHM values in the flat region of the curves shown in Fig 3a) is 0.5%, 2% and 0.1% for *x*, *y* and *z*. If the FWHM is measured along one of the low resolution directions, instead of the high resolution one, a 100% change is observed with increasing voxel size as expected, Fig. 3b). Fig 3c) shows the directional dependence of the FWHM calculated from a scan with a matrix size of 32^3. The scan was acquired obliquely, with a 30º tilt relative to the *x*-*z* plane. The tilt measured from Fig 3c) is 32º demonstrating that a lower resolution scan can be used to initially determine the principal directions to be used for FAAR measurements of the principal values.

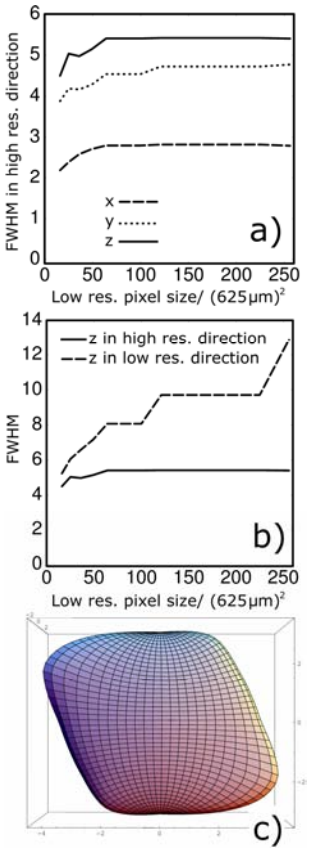

Figure 3. a) FWHM of the ACF measured along the *x*, *y* and *z* gradient axis at different resolutions in the *y*-*z*, *x*-*z* and *x*-*y* plane respectively. The principal axes of the phantom were parallel to the gradient axes. b) FWHM of the ACF along the *z*-direction as measured with a high (solid line) and a low (dashed line) resolution acquisition along the *z*-axis. c) A 3 dimensional rendering of the directional dependence of the FWHM as measured from a lower, isotropic resolution scan. The measured tilt of the principal axes is 32° in agreement with the experimentally prescribed 30º.

Research funded by NIH grants T32EB000814 and RO1 49553.

[1] C. H. Turner, J. Biomech. 25: 1-9, 1992; [2] S. N. Hwang et al, Med Phys. 24: 1255, 1997;